Validation of tissue-specific RNAi systems in *C. elegans* reveals a converging role for polyubiquitin UBQ-1/UBC in vitellogenin metabolism and lifespan

Noeli Soares Melo da Silva[1,2], Cristina Bolonyi[1,2,#], Adia Ouellette[1,2,#], Laura Harrison[1,2,#], Sung Youn Kim[1,2], Sandrine Daigle[1,2], Savannah T. Doucet[1,2], Louis R. Lapierre[1,2,*]

[1] New Brunswick Centre for Precision Medicine, 27 Providence Street, Moncton, Canada E1C8X3

[2] Chemistry and Biochemistry Department, Université de Moncton, 18 Antonine Maillet, Moncton, Canada E1A3E9

[#] Equal contributors

* Corresponding author

ABSTRACT

Numerous studies in *C. elegans* have taken advantage of gene silencing RNAi libraries and tissue-specific RNAi systems to temporally and spatially understand gene function. Tissue-specific RNAi strains were created via tissue-specific functional expression of a key gene in the RNAi system in a presumably RNAi insensitive correspondingly-mutated background. Here, we tested the level of RNAi insensitivity across different commonly used RNAi-defective mutants (*rde-1* and *sid*-1) using lifespan analyses. Remarkably, while we found similarly important lifespan shortening in wild-type animals by silencing the polyubiquitin gene *ubq-1* (*UBC*) at both 20°C and 25°C, we found wide and temperature-sensitive variations in RNAi sensitivity across different *rde-1* and *sid-1* strains from substantial sensitivity to complete insensitivity. This riveting finding warrants a re-evaluation of the tissue-specific interpretations in numerous tissue-specific RNAi

studies in *C. elegans*. Using validated tissue-specific RNAi systems, we determined that proteasomal burden largely differs between the germline and the soma. Notably, gonadally-accumulating vitellogenin proteins substantially contributed to the total polyubiquitinated proteins observed during aging. Interestingly, we found that UBQ-1 was essential to maintain the transcription of highly expressed genes, including vitellogenins, supporting a broad and key role for polyubiquitin beyond proteostasis. Altogether, we authenticated commonly used tissue-specific RNAi systems and uncovered a new approach to improve RNAi insensitivity in RNAi-defective strains. With validated tissue-specific RNAi strains, we spatially analyzed proteasomal function and age-related polyubiquitinated protein accumulation, and revealed a converging regulatory link between UBQ-1, vitellogenin metabolism and lifespan in *C. elegans*.

INTRODUCTION

The advent of mRNA silencing with interfering RNA (RNAi) from bacterially-expressed double-stranded RNA empowered researchers to investigate specific and temporal control of gene expression in *C. elegans*, opening the door to studies of gene function across life stages [1]. This innovation also avoided ambiguous interpretations of adult-specific gene function when corresponding mutants have developmental issues. Genome-wide RNAi libraries from the Ahringer [2] and Vidal [3] laboratories were instrumental in providing broad and complementary coverage for gene silencing. Unbiased genome-wide RNAi screen, such as the ones performed to discover lifespan-modulating genes [4, 5], delivered an incredible wealth of information about genetic determinants of longevity and aging [6, 7].

47 Broad interest in understanding tissue-specific gene function in *C. elegans* eventually led
48 to the development of strains that enable gene silencing in only one tissue. These strains
49 were constructed in RNAi-defective mutants whereas functional reconstitution of the
50 defective gene under a tissue-specific promoter would restore RNAi sensitivity in a tissue-
51 specific manner. Three essential considerations needed to be met to allow tissue-specific
52 RNAi strains to provide valid and rigorous interpretations of tissue-specific gene function.
53 First, the RNAi-defective mutants needed to be entirely insensitive to RNAi as any
54 remaining sensitivity will mislead interpretation. Mutations of the *rde-1* gene coding for a
55 key protein in the RNA-induced silencing complex (RISC) complex [8] or mutations of the
56 *sid-1* gene coding for the dsRNA channel necessary for dsRNA import into tissues [9]
57 were generally selected to construct tissue-specific strains. Second, the tissue-specific
58 promoter used to drive the expression of the functional gene had to be exclusively
59 restricted to the tissue of interest [10]. Third, the 3'UTR regions in the expression plasmid
60 needed to be compatible with the targeted tissue for reconstitution. This could be typically
61 addressed by matching the promoter with the corresponding 3'UTR [11]. Ideally, such
62 reconstitution would have restricted gene silencing in only a specific tissue and provided
63 a tool to analyze tissue-specific gene function.
64
65 Clear warning signs emerged over the past decade about the rigor and reproducibility of
66 tissue-specific RNAi strains developed in *C. elegans*, including not only the use of *rde-1*
67 and *sid-1* mutant strains [12, 13] but also the use of mutants of the RNA-dependent
68 polymerase *rrf-1* for germline-specific RNAi [14]. Regrettably, tissue-specific RNAi
69 systems were initially designed on the unsubstantiated assumptions that RNAi-

70 defectiveness equals completely insensitivity to RNAi and that certain promoters can
71 drive the expression of function genes (such as RDE-1 or SID-1) in just one specific tissue
72 [15]. Astonishingly, despite being used in hundreds of publications, systematic
73 demonstration of the validity of different tissue-specific RNAi strains has been lacking.
74
75 One area of research where identifying the function of genes in a tissue-specific manner
76 would meaningfully advance our understanding is the field of proteostasis and aging. For
77 instance, complementary strategies (including tissue-specific reconstitutions and auxin-
78 degradation systems) have identified tissue-specific roles for the proteostasis-related
79 transcription factor DAF-16/FOXO in the longevity mechanism of long-lived animals such
80 as the Insulin-IGF-1 receptor *daf-2* mutants [16-18]. However, the tissue-specific role of
81 key mechanisms in the proteostasis network, such as the 26S proteasome, remain
82 incompletely understood. The 26S proteasome is a major degradation machinery of
83 polyubiquitinated proteins [19], and aging *C. elegans* progressively accumulate
84 proteasomal subunits, perhaps in a futile attempt to prevent further protein aggregation
85 [20] that ultimately characterizes the age-related proteostatic collapse [21, 22]. Subunits
86 in the 26S proteasome have been linked to lifespan determination [23, 24], but the tissue-
87 specific contributions of proteasomal degradation in longevity are unclear and the tissue-
88 specific dynamics of polyubiquitinated proteins is unknown.
89
90 Here, we systematically validated commonly used tissue-specific RNAi systems in *C.*
91 *elegans* and found that the level of RNAi insensitivity of RNAi-defective strains and the
92 level of specificity of tissue-specific RNAi strains unexpectedly vary widely. We uncovered

that increasing temperature could improve RNAi insensitivity in some RNAi-defective mutants, potentially via further structural destabilization from point mutations. Leveraging validated tissue-specific RNAi strains, we identified the germline as a key tissue for proteasomal degradation, markedly overshadowing somatic tissues in proteasomal polyubiquitinated protein burden. We found that such burden is due in part by germline-acquired vitellogenins that are actively degraded during embryogenesis. We demonstrate the requirement for rigorous protein extraction protocols in the study of polyubiquitinated proteins during aging in *C. elegans* [25], including the use of aggregate-solubilizing buffers, and we highlight the need to study somatic and germline proteostasis separately in *C. elegans*. Finally, we uncover a novel role for the polyubiquitin gene *ubq-1* in the regulation of highly expressed genes including vitellogenins, suggesting a converging regulatory role for polyubiquitin in vitellogenin metabolism and lifespan.

RESULTS

RNAi-defectiveness of *rde-1* and *sid-1* mutants varies greatly and is modulated by temperature.

Many RNAi-defective mutants (including *rde-3, rde-4, rde-10* and *rde-11*) retain RNAi sensitivity during short-term silencing, preventing their use to develop tissue-specific RNAi systems [12]. To unambiguously determine RNAi insensitivity, we tested the effect of whole-adulthood RNAi treatments in commonly used RNAi-defective mutants, including two *rde-1 (ne300* and *ne219)* [8] and two *sid-1 (qt9* and *pk3321)* mutants that have established transgenic tissue-specific RNAi reconstitutions (**Supplementary Table S1**). To ensure that gene silencing provokes a remarkable effect on lifespan, we opted to

116 silence *ubq-1,* a well-conserved gene (UBC in humans) encoding polyubiquitin [26].
117 Silencing *ubq-1* in wild-type N2 animals led to a marked mean lifespan decrease of about
118 50-60% at 20°C (**Figure 1A, Supplementary Table S2**). In different commonly used
119 RNAi-defective mutants, silencing *ubq-1* at 20°C had surprisingly variable effects.
120 Interestingly, the lifespan of *rde-1(ne300)* was not affected by whole adulthood *ubq-1*
121 silencing highlighting that they are indeed RNAi-insensitive (**Figure 1B**). Indeed, levels of
122 *ubq-1* mRNA are not decreased in *rde-1(ne300)* subjected to *ubq-1* RNAi
123 (**Supplementary Figure S1A).** This is in line with previous observations of the lack of
124 short-term RNAi effects when silencing fatty acid desaturases in *rde-1(ne300)* mutants
125 [12], and confirms the functional abrogation of RDE-1 from this premature stop codon
126 mutation. However, in *rde-1(ne219), sid-1(qt9)* and *sid-1(pk3321)* mutants (all point
127 mutations), *ubq-1* silencing resulted in significant deleterious effects on lifespan,
128 indicating functionally hypomorphic variants that are not insensitive to RNAi at 20°C
129 (**Figure 1C-E, Supplementary Table S2**). Since most studies in *C. elegans* are generally
130 performed at 20°C, our data demonstrates that using RNAi-defective, but not fully RNAi-
131 insensitive strains to study tissue-specific effects prevents appropriate interpretations.
132
133 Since increasing temperature can affect the extent of the loss of function in mutants [27],
134 we performed comparative lifespan analyses at 25°C in RNAi-defective mutants. Akin to
135 20°C, *ubq-1* silencing at 25°C resulted in a mean lifespan decrease of approximately 50%
136 (**Figure 1F, Supplementary Tables S3**). This demonstrates that the capacity of the RNAi
137 machinery to perform gene silencing was not affected by temperature, and the impact of
138 silencing *ubq-1* on lifespan was correspondingly scaled between 20°C and 25°C [28, 29].

139 Expectedly, the *rde-1(ne300)* mutants remained insensitive to RNAi at 25°C (**Figure 1G,**
140 **Supplementary Table S2**). Interestingly, silencing *ubq-1* in *rde-1(ne219)* mutants at 25°C
141 did not affect their lifespan, indicating that the *rde-1(ne219)* point mutation becomes null
142 at that temperature (**Figure 1H, Supplementary Table S2**). Since the hypomorphic loss
143 of function at 20°C becomes null at 25°C in the *rde-1(ne219)* background, this strain could
144 technically be used at 25°C for testing tissue-specific RNAi, resolving previous concerns
145 for this strain in tissue-specific RNAi reconstitutions [12]. Increasing temperature to 25°C
146 reduces the impact of *ubq-1* silencing on the lifespan of *sid-1(qt9)* and *sid-1(pk3321)*,
147 suggesting that RNAi-sensitivity in these two mutants is also temperature-sensitive
148 (**Figure 1I-J, Supplementary Table S2**). At both 20°C and at 25°C, *sid-1(qt9)* as well as
149 in germline-less *sid-1(qt9);glp-1(e2144)* mutants remained sensitive to RNAi
150 (**Supplementary Tables S2 and S3**). Moreover, *sid-1(pk3321)* mutants still retained
151 significant RNAi sensitivity at 25°C (**Figure 1J**), corroborating a recent report highlighting
152 this commonly used strain as incompatible for testing tissue-specific role of genes with
153 RNAi [13]. Overall, our data indicates that only *rde-1(ne300)* is a suitable background at
154 both 20°C and 25°C for interpreting tissue-specific RNAi strains, and we recommend
155 experimenting at 25°C when using tissue-specific strains constructed from *rde-1(ne219)*
156 mutants.
157
158 To investigate the structural impact of the *rde-1* and *sid-1* variants studied, we performed
159 an *in silico* comparative analysis of the *rde-1* and *sid-1* proteins using UCSF ChimeraX
160 [30]. Wild-type reference structures, obtained from the AlphaFold Database and the PDB
161 (ID: 8XC1), were superimposed with mutant models generated via the AlphaFold server.

162 The superposition analysis demonstrated that the global architecture of the proteins
163 remains highly conserved across all variants, with minimal deviations in the polypeptide
164 backbone (**Figure 2A-C**). The RMSD value obtained for the pruned atom pairs in *rde-1*
165 was 0.845 Å, while the values for *sid-1* (*qt9*) and *sid-1* (*pk3321*) relative to the wild-type
166 protein were 1.006 Å and 0.978 Å, respectively. However, detailed examination of the
167 substitutions revealed significant local changes at the mutation sites: the E414K
168 substitution in *rde-1(ne219)* resulted in the replacement of an acidic residue with a basic
169 one (**Figure 2A**). In *sid-1(qt9) and sid-1(pk3321)*, the S536I and D130N mutations
170 promoted, respectively, the introduction of a hydrophobic residue into a polar region and
171 a charge alteration in the extracellular domain (**Figure 2B-C**). These structural predictions
172 suggest that the observed phenotypic dysfunctions arise from local electrostatic or
173 hydrophobicity changes rather than a collapse of the primary protein folding. Increased
174 temperature likely further destabilizes those key functional regions, ultimately reducing
175 RNAi sensitivity. Taken together, our lifespan analyses clearly demonstrate that proper
176 validation of RNAi-defective strains in the development of tissue-specific RNAi systems
177 is essential. By increasing temperature to 25°C, we also uncovered that RNAi insensitivity
178 can be fully attained in *rde-1(ne219)* mutants and can be partially improved in *sid-1(qt9)*
179 and *sid-1(pk3321)* mutants, likely via functionally relevant local structural destabilization.
180

181 **Tissue-specific RNAi strains are not always specific to their corresponding tissue**

182 Despite numerous publications, authentic specificity of commonly used tissue-specific
183 RNAi strains has never been fully characterized. Thus, we tested the specificity of
184 previously engineered tissue-specific RNAi strains in both *rde-1* and *sid-1* background

185 [31-38] (**Supplementary Table S1**). To test the level of tissue-specificity, we leveraged
186 important tissue-specific genes that create unequivocal morphological or behavioral
187 changes in 100% of wild-type animals when silenced during development. For the
188 intestine, we silenced *elt-2*, a transcription factor involved intestinal development and
189 differentiation [39]. Loss of *elt-2* leads to underdeveloped and clear larvae. For the
190 hypodermis, we silenced *bli-3*, an NADPH oxidase essential for molting, whereas its loss
191 leads to a short animal with blisters [40]. For the muscle, we silenced *unc-54*, a myosin
192 gene necessary for muscle function and mobility [41]. For the germline, we silenced *xpo-*
193 *1,* a nuclear exportin important in germline development and lifespan [42, 43]. Low *xpo-1*
194 during development affects the reproductive system and leads to curled adult animals
195 and vulvar protrusion [42]. We silenced these genes in commonly used tissue-specific
196 RNAi systems generally available at the Caenorhabditis Genetics Center (CGC)
197 (**Supplementary Table S1**). Importantly, since the silencing was done on a short period
198 of time (i.e. eggs to day 1 of adulthood), unlike our adult-only silencing lifespan analyses
199 (**Figure 1A-J**), we did not observe any deleterious effect of tissue-specific RNAis in RNAi-
200 defective strains, indicating that short periods of silencing may not suffice to
201 phenotypically observe RNAi sensitivity in those strains (**Figure 3A-D**). We found that in
202 *rde-1(ne300)* background [12], every tissue-specific RNAi strain behaved as advertised
203 (**Figure 3A-D**). Notably, silencing *elt-2* in strains with intestinal RNAi sensitivity
204 reproducibly generally resulted in 100% of animals displaying clear developmental
205 deficits. In the *rde-1(ne219)* background, the annotated intestine-specific RNAi strain was
206 also sensitive, albeit partially, to hypodermal gene silencing (**Figure 3A-D**). Although
207 unclear, different extents of phenotypic representation could be due to varying levels of

208 exposure of bacteria expressing dsRNA on agar plates. The annotated hypodermal-
209 specific RNAi strain was also sensitive to intestinal and germline-related gene silencing
210 (**Figure 3A-D**). The muscle-specific RNAi strain had RNAi sensitivity in muscle, but with
211 relatively low silencing capacity (**Figure 3A-D**). The germline-intestine-specific and the
212 germline-specific strains were limited to their annotated tissues (**Figure 3A-D**).
213
214 In the *sid-1(qt9)* background, some tissue-specific reconstitutions also include a co-
215 expressed fluorescent marker driven by the corresponding promoter to help visualize
216 tissue-specificity (**Supplementary Table S1**). However, as observed with the *mtl-2*
217 promoter in the *rde-1(ne219)* background, the intestine-specific RNAi strain designed with
218 the *gly-19* promoter displayed partial RNAi sensitivity to *bli-3* silencing (**Figure 3A-D**). On
219 the other hand, the muscle-specific strain was only sensitive in the muscle (**Figure 3A-**
220 **D**). Neuronal-specific strains were not RNAi sensitive in peripheral tissues (**Figure 3A-**
221 **D**), which differs from the strains originally built from *sid-1(pk3321)* [13]. Taken together,
222 our analysis of tissue-specificity clearly lays out the limitations associated with
223 reconstituting gene function under a particular promoter and highlights the importance of
224 proper validation of commonly-used tissue-specific RNAi-sensitivity reconstitutions prior
225 to experimentation.
226
227 **Proteasomal degradation is most active in the germline**
228 One of the leading questions in *C. elegans* aging studies is: how does the proteostasis
229 network changes during aging? Longitudinal proteomic analyses in different nematodes
230 have suggested that subunits of the 26S proteasome accumulate during aging [20], but

231 their impact on overall polyubiquitinated protein metabolism is unclear. The 26S
232 proteasome, which consists of a 19S cap and 20S proteolytic core, carries out the
233 degradation of most polyubiquitinated proteins. Unexpectedly, in short-lived
234 proteostatically-deficient *C.* elegans, including *hlh-30(tm1978)* [44], *hsf-1(sy441)* [45] and
235 *daf-16(mu86)* [46], total levels of polyubiquitinated proteins did not significantly change at
236 day 1 of adulthood (**Supplementary Figure S1B**). In wild-type *C. elegans*, we observed
237 that the levels of polyubiquitinated proteins remains elevated during aging, using a
238 complete solubilization protocol to avoid missing age-related protein aggregates
239 (**Supplementary Figure S1C-F**). Thus, age-related accumulation of 26S proteasomes
240 [20] does not seem to markedly affect overall levels of polyubiquitinated proteins.
241 Seemingly, the steady-state total polyubiquitinated protein levels may not be a correlate
242 of the overall status of the proteostasis network in different nematodes.
243
244 While many proteins are polyubiquitinated in *C. elegans*, the tissue-specific contribution
245 of the total polyubiquitinated protein pool remains unknown. Using the established and
246 broad tissue-specific RNAi system in the *rde-1(ne219)* background (**Supplementary**
247 **Table S1**), we tested the role of the proteasome on polyubiquitinated protein
248 accumulation by silencing 19S-related gene *rpn-6* and 20S-related gene *pas-7* [47] in
249 tissue-specific strains validated in **Figure 2**. We also silenced *ubq-1* to better understand
250 the role of polyubiquitin in different tissues. In wild-type animals, loss of proteasome led
251 to a marked increase in total polyubiquitinated proteins, particularly in the higher
252 molecular weight range, which was accompanied by increases in vitellogenin protein
253 levels (**Figure 4A**, vitellogenins * and **) as observed by ponceau staining (antibodies for

254 vitellogenins are unavailable). Six forms of vitellogenins exist, *vit-1* to *vit-6*, and they are
255 the most abundant family of proteins in *C. elegans*, accounting for almost 20% of the total
256 proteome [43]. While *vit-1* to *vit-5* are similar and overlap at 170kDa (*), *vit-6* is processed
257 in two polypeptides of 115 and 88 kDa (**). Loss of *ubq-1* abolishes the presence of
258 polyubiquitinated proteins, and surprisingly, led to a complete loss of vitellogenin proteins
259 (**Figure 4A**). Conversely, RNAi-defective *rde-1(ne219)* mutants did not respond to any
260 RNAi treatment. In tissue-specific RNAi-sensitive reconstitution in the intestine and
261 germline, we surprisingly saw limited increases in polyubiquitinated protein, suggesting a
262 relatively limited role for the 26S proteasome in these tissues in the turnover of
263 polyubiquitinated proteins. In tissue-specific RNAi reconstitution in intestine, hypodermis
264 and germline or intestine and germline, we observed similar vitellogenin and
265 polyubiquitinated protein accumulation found in wild-type animals (**Figure 4D-E**),
266 suggesting that the germline may be an important proteasomal degradation site. To
267 directly confirm this, we silenced proteasome-related genes in a germline-specific RNAi
268 reconstitution and found that limiting silencing to the germline is sufficient to accumulate
269 polyubiquitinated proteins to a similar level than wild-type animals (**Figure 4F**). This
270 demonstrates the unique and important role of proteasomal function in the germline and
271 puts into context previous use of total polyubiquitinated protein levels as a proxy for
272 organismal proteostasis. Here, we find that the extent of germline-specific and somatic
273 proteasomal function markedly differs, a previously unrecognized difference that reveals
274 important limitations in globally and indiscriminately studying polyubiquitinated protein
275 metabolism and dynamics while inhibiting the proteasome systematically.
276

277 **Vitellogenin proteins in the germline are important contributors of total**
278 **polyubiquitinated proteins**

279 The inhibition of proteasomal function in the germline increased the levels of
280 polyubiquitinated proteins and vitellogenins, and inhibition in the intestine and hypodermis
281 had minimal impact on polyubiquitinated protein accumulation (**Figure 4D-F**). Thus, we
282 reasoned that vitellogenin proteins, synthesized in the intestine and secreted thereafter,
283 may be readily subjected to polyubiquitination only after entering the gonad, ultimately
284 providing amino acids and lipids to oocytes via delipidation and proteasomal degradation.
285 Here, we assessed the levels of total polyubiquitinated proteins at day 1 of adulthood in
286 wild-type animals, *fer-15(b26);fem-1(hc17)* mutants that are sterile at 25°C and *glp-*
287 *1(e2144)* mutants that are devoid of a germline at 25°C. Compared to wild-type animals,
288 *fer-15;fem-1*mutants accumulated more polyubiquitinated proteins, which may suggest a
289 tendency for these sterile animals to trap larger amounts of vitellogenin proteins in the
290 unfertilized oocytes (**Figure 5A**). Conversely, since they lack a germline, *glp-1* mutants
291 do not accumulate vitellogenin in the reproductive tissue due to its absence and of low
292 expression of the vitellogenin endocytosis receptor *rme-2* [48, 49]. Germline-less animals
293 carry significantly less polyubiquitinated proteins, despite having elevated vitellogenin
294 accumulation, which is largely pseudocoelemic [49, 50] (**Figure 5A**). Since both sterile
295 *fer-1;fem-15* and germline-less *glp-1* animals have dysfunctional reproductive systems,
296 the levels of polyubiquitinated proteins remain largely the same later in adulthood (**Figure**
297 **5B**). Unexpectedly, silencing proteasomal subunits in *glp-1* animals did not result in
298 overly large accumulation of polyubiquitinated proteins (**Figure 5C**), as seen in wild-type
299 animals (**Figure 4A**). This observation combined with our data in intestine-hypodermis

300 RNAi sensitive strain (**Figure 4C**) is rather perplexing considering the previously
301 highlighted role for proteasomal function in the intestine of long-lived *glp-1* animals [23],
302 and suggest relatively limited burden of the 26S proteasome in the soma compared to the
303 germline. Using animals expressing VIT-2::GFP [48], we found that silencing *rpn-6* led to
304 marked accumulation in the reproductive system while silencing *ubq-1* abrogated VIT-
305 2::GFP levels (**Figure 5D**), corroborating our observations by ponceau (**Figure 4A**).
306
307 To directly determine the role of germline-located vitellogenins in the total
308 polyubiquitinated pool, we silenced the vitellogenin endocytosis receptor *rme-2* [48] as
309 well as vitellogenins using *vit-1* RNAi as it efficiently silences all vitellogenins [49]. Lower
310 total polyubiquitinated proteins were observed when transport of vitellogenins to the
311 gonad is abrogated or when vitellogenins are silenced (**Figure 5E**). This is in line with
312 previous proteomic analyses demonstrating the presence and accumulation of
313 ubiquitinated vitellogenins in *C. elegans* [51]. Finally, in extracted gonadal tissue from
314 wild-type animals, we observed ubiquitin-rich cytoplasmic clusters in developing oocytes,
315 suggesting that the germline contains ample cargos, including vitellogenins, for
316 proteasomal degradation (**Figure 5F**). This is supported by the presence of noticeably
317 bright eggs layed by VIT-2::GFP expressing animals when proteasomal subunit *rpn-6* is
318 inhibited (**Figure 5D,** arrow). Taken together, our data support a key role for the
319 proteasome in vitellogenin metabolism in the germline, and an important contribution for
320 gonadally-located vitellogenins in overall polyubiquitinated protein levels in *C. elegans*.
321
322 **UBQ-1 is essential for the transcription of highly-expressed genes**

323 Our tissue-specific strain analysis of proteasome function inadvertently revealed a role
324 for UBQ-1 in vitellogenin production (**Figure 4A-F**). Indeed, *ubq-1* silencing led to an
325 almost complete abrogation of vitellogenin in animals sensitive for RNAi in the intestine
326 (**Figure 4A,C-E**) while having no effect in the germline-specific RNAi strain (**Figure 4F**).
327 Vitellogenins are the most abundant proteins and among the most expressed genes in *C.*
328 *elegans* [43] and since they generally are secreted after being synthesized in the
329 intestine, we reasoned that the significant reduction in vitellogenins may be due to a
330 marked decrease in synthesis accompanied by secretion of existing vitellogenins and
331 subsequent loss when eggs were laid. In addition to ponceau (**Figure 6A**), we observed
332 the loss of vitellogenin with a VIT-2::GFP reporter when *ubq-1* was silenced (**Figure 5D**).
333 To systematically understand the role of UBQ-1 in transcription, we silenced *ubq-1* during
334 early adulthood and identified the global transcriptomic changes by RNA sequencing
335 (**Supplementary Figure S2A-B, Supplementary Data S1**). Loss of *ubq-1* led to a drastic
336 transcriptional rearrangement and pathway enrichment analysis suggested major
337 downregulation of metabolic and stress response genes (**Figure 6B-C**). Interestingly, we
338 found a massive reduction of many of the highest transcribed genes, with the largest
339 downregulations featuring vitellogenin genes (**Figure 6D**). This indicated a key role for
340 UBQ-1, not only in lifespan, but also in the active transcription of highly expressed genes.
341 Taken together, our study demonstrates roles for the polyubiquitin gene UBQ-1 that
342 extends beyond proteostasis to transcriptional specification and converges to modulate
343 vitellogenin metabolism and lifespan.
344

345 **Discussion**

346 Significant advances have been made over the last decade to develop tools for spatial
347 and tissue-specific study of the role of genes in *C. elegans* biology. Unfortunately, a
348 complete validation of available tissue-specific RNAi systems over the lifespan of *C.*
349 *elegans* had yet to be performed. Even after several years and hundreds of publications,
350 proper demonstration of RNAi insensitivity in RNAi-defective mutants remained an
351 important validation of tissue-specific RNAi systems allowing proper studies of tissue-
352 specific function of genes in *C. elegans*. Here, we thoroughly determined the validity of
353 different RNAi-defective strains for the development and use of tissue-specific RNAi
354 strains.
355
356 Leveraging the efficient lifespan-shortening effects of silencing polyubiquitin gene *ubq-1,*
357 *w*e found that *rde-1(ne300)* is a robust strain beyond short-term silencing [12] and across
358 the whole lifespan of *C. elegans*. Corresponding tissue-specific strains were also
359 restricted for RNAi sensitivity to their specific tissue. We uncovered that the *rde-1(ne219)*
360 are only fully insensitive to RNAi at 25°C, supporting a temperature-sensitive null mutation
361 via local structural destabilization at the point mutation. Our whole adulthood silencing
362 approach strengthen our understanding of RNAi-defective strains from short-term RNAi
363 studies [31, 52] and provide unequivocal answers on the RNAi insensitivity necessary for
364 the construction of tissue-specific RNAi system. Notably, tissue-specific RNAi strains in
365 the *rde-1(ne219)* and *sid-1(qt9)* originally identified for the intestine or the hypodermis,
366 but sensitive in either tissue or more, will need to be re-annotated accordingly. Finally, we
367 conclude that the *sid-1(qt9)* and *sid-1(pk3321)* mutants are ill-suited for the development
368 of tissue-specific RNAi strains, because they retain substantial long-term RNAi capacity

369 at both 20°C and 25°C. While our tissue-specific validation of RNAi systems using short-
370 term silencing suggest that tissue reconstitutions in *sid-1(qt9)* mutants are generally
371 robust, studies using long-term silencing are not advisable in that background.
372 Additionally, tissue-specific reconstitution of SID components was recently shown to
373 negatively affect lifespan [53]. Therefore, the numerous studies using *sid-1(qt9)* and *sid-*
374 *1(pk3321)* and the corresponding tissue-specific reconstitutions should be re-evaluated
375 with our observations in mind. Altogether, our study systematically clarified the issues
376 related to the development and use of tissue-specific strains in *C. elegans* and uncovered
377 a solution (i.e. experiments carried out at 25°C) to address incomplete RNAi insensitivity
378 in *rde-1(ne219)* mutants at 20°C.
379
380 The role of the 26S proteasome in the lifespan of *C. elegans* and the dynamics of
381 polyubiquitinated proteins have been previously highlighted [23, 24, 51], but tissue-
382 specific contributions were unclear and proper polyubiquitinated protein analyses that
383 included aggregated proteins were lacking. Here, we uncovered an important role for the
384 26S proteasome in the germline, especially in the metabolism of polyubiquitinated
385 vitellogenin proteins. Germline-specific silencing of 26S proteasome subunits led to
386 similar accumulation of polyubiquitinated proteins to whole-organism silencing,
387 demonstrating that whole-organism analyses of polyubiquitinated proteins is relatively
388 misleading, especially when trying to study somatic maintenance and longevity. This is
389 particularly evident when levels of polyubiquitinated proteins are analysed longitudinally
390 (**Supplementary Figure S1C-F**) and comparatively in different short-lived, sterile and
391 germline-less animals (**Figures 5A and Supplementary S1B**). Indeed, total levels of

392 polyubiquitinated proteins in *C. elegans* are an incomplete proxy for the organismal-wide
393 status of the proteostasis network.
394
395 In our study, we find that the key converging feature for polyubiquitinated protein
396 accumulation in *C. elegans* is vitellogenin metabolism in the germline. As observed in
397 germline-less animals that accumulate vitellogenin proteins in the pseudocoelom [49, 50],
398 intestinally synthesized vitellogenins are likely only ubiquitinated when it reaches the
399 gonads. Vitellogenin structure, homologous to the N-terminus of human apolipoprotein B
400 (apoB), is a large lipid transfer protein with amphipathic beta-sheets that accommodate
401 lipids to a high-density lipoprotein level [54]. The relatively compact structure of
402 vitellogenins accompanied by co-translational lipidation in the endoplasmic reticulum
403 generally protects nascent lipoproteins from co-translational ubiquitination observed with
404 the significantly larger and more hydrophobic apoB protein [55]. However, endocytosis in
405 the germline and transport to developing embryos likely destabilizes vitellogenins,
406 fostering their ubiquitination [51] and consequent proteasomal degradation. In *Caurosius*
407 *morosus* (stick insect) vitellin, a processed formed of vitellogenin, is ubiquitinated and
408 degraded in the developing embryos [56]. We previously found that lipid-droplet enriched
409 fraction contains high levels of polyubiquitinated proteins when *rpn-6* is silenced, and a
410 portion of that accumulation may be related to germline-associated vitellogenins [57].
411 Thus, we conclude that vitellogenins are ubiquitinated in the germline, potentiated by
412 destabilization as it enters the germline and as its lipids gets progressively mobilized by
413 the developing embryos. The appearance of undegraded vitellogenin proteins in laid eggs
414 when proteasomal function is inhibited supports this mechanism (**Figure 5D**).

415

416 Vitellogenin protein degradation dynamics in the germline could therefore largely account
417 for variations in total polyubiquitinated protein levels in different *C. elegans* strains. In
418 wild-type animals (and in short-lived animals), brood size is similar and brood production
419 ends within the first 5 days of adulthood. In *fer-15;fem-1* sterile animals, the inability to
420 generate viable progeny leads to increased accumulation of polyubiquitinated proteins in
421 the germline. Proteostasis challenges associated with sterility have been previously
422 reported [58]. The role of the 26S proteasome in the germline was also recently
423 highlighted in the context of sex determination and transgenerational information transfer
424 [59]. The rate of progeny production likely also plays a role in determining steady-state
425 total polyubiquitinated protein levels. Reported vulvar venting of vitellogenins from adults
426 to progenies could conceivably contribute to fluctuations in total polyubiquitinated proteins
427 [60]. Overall, our data points to important tissue-specific variations in proteasomal burden,
428 especially between the germline and the soma, and centers vitellogenins as important
429 contributors to total observed polyubiquitinated proteins in *C. elegans*.

430

431 The polyubiquitin gene UBQ-1/UBC is important for normal lifespan in *C. elegans* [61],
432 and its role in proteostasis is well established [62]. When expressed, this polyubiquitin
433 protein gets cleaved by UBC hydrolases to form ubiquitin available for the ubiquitin-
434 proteasome system [63]. Ubiquitin can also serve as a transcriptional activator or
435 repressor when conjugated with histones, affecting chromatin compaction and promoter
436 accessibility [64, 65]. Here, we found that loss of *ubq-1* generates important and broad
437 transcriptional changes that likely contribute to the accelerated aging observed.

438 Interestingly, despite being highly expressed throughout adulthood, vitellogenins are
439 among the most downregulated genes from the loss of *ubq-1*, highlighting the major role
440 of ubiquitin on highly active transcription. Because of the massive downregulation of those
441 genes, ubiquitin may be essential for the transcriptional machinery to access those
442 corresponding. Alternatively, ubiquitin-dependent chromatin dynamics on typically
443 repressed gene loci may be lost potentially leading to re-positioning of transcription
444 factors and machineries onto typically lowly-expressed genes, thereby minimizing the
445 expression of otherwise highly expressed genes. As aging is characterized by progressive
446 transcriptional drift due in part by age-related epigenetic changes [66, 67], our study
447 positions the maintenance of UBQ-1 expression and function as a key proteostatic and
448 transcriptional modulator in the health and lifespan of *C. elegans*.
449
450 Importantly, our study demonstrates the importance of proper initial validation of tools to
451 study gene function, in particular tissue-specific RNAi systems. We conclude that the use
452 of *rde-1* strains to construct tissue-specific strains is a superior approach to the use of
453 *sid-1* strains. Here, we also provide an optimized protocol for the analysis of
454 polyubiquitinated proteins, with a focus on complete homogenization to help reach whole
455 proteome analyses and improve interpretations. Our original goal of authenticating tissue-
456 specific RNAi strains led us to uncover major differences in proteasomal function between
457 the soma and the germline, placing vitellogenins as important polyubiquitinated targets in
458 developing embryos. Finally, we inadvertently uncovered that the polyubiquitin gene
459 UBQ-1 is an essential protein in the proper maintenance of transcription, especially of

460 highly-expressed genes such as vitellogenins, placing it as a converging modulator of
461 vitellogenin metabolism and lifespan.
462
463 **METHODS**
464 ***C. elegans* maintenance, growth and visualization**
465 Strains of *C. elegans* were grown and maintained at 20°C on growth media agar plates
466 seeded with *E. coli* strain OP50 and handled as previously described [68]. Ethical
467 approval was not required for nematode experiments by our institution. Strains used in
468 this study are listed in **Supplementary Table S1**. For imaging, nematodes were
469 immobilized with 0.1% sodium azide and visualized with a V20 fluorescence
470 stereomicroscope (Zeiss). Exposure and magnification were maintained between
471 conditions.
472
473 **Lifespan analyses and silencing experiments**
474 Nematodes were synchronized by hypochlorite treatment and grown at 20 °C or 25 °C on
475 *E. coli* OP50 until the first day of adulthood. Animals were then maintained at the same
476 temperatures on plates seeded with either control bacteria (*E. coli* HT115 carrying the
477 L4440 empty vector) or bacteria producing double-stranded RNA (dsRNA) targeting the
478 *ubq-1* gene (Ahringer library) [2]. Animal survival was assessed every 2–3 days and
479 tissue-specific silencing was performed using RNAi against *elt-2* (Ahringer library), *bli-3*
480 (Vidal library), *unc-54* (Ahringer library), *xpo-1* (Ahringer library). Graphs were created
481 using OriginPro 9 (OriginLab) and statistical analyses (Mantel-Cox log-rank) were
482 performed using the OASIS 2 (https://sbi.postech.ac.kr/oasis2/surv/).

483

484 **Protein solubilization for immunoblotting**

485 To completely solubilize proteins, we used a RIPA solution (50mM Tris-HCl, 150mM NaCl,
486 1mM EDTA, Roche Complete Protease Inhibitors) containing 5% SDS followed by
487 heating for 5 minutes at 95°C and sonication for 20 seconds (QSonica Q55, 30% input).
488 Insoluble proteins were pelleted by centrifugation for 2 minutes at 12000rpm. This first
489 solubilization step (250μl of 5% SDS-RIPA) solubilized over 90% of total proteins, and a
490 second step of solubilization (250μl of 5% SDS-RIPA) successfully solubilized the small
491 pellet. Ubiquitinated proteins from combined (i.e. total) were visualized by
492 immunoblotting. Mild homogenization (MH) was also performed using the buffer (250μl)
493 and method described in Koyuncu et al. [51] and insoluble proteins were pelleted by
494 centrifugation for 2 minutes at 12000rpm. Subsequently, these larger pellets (compared
495 to the 5% SDS-RIPA method) were completely solubilized with 5% SDS-RIPA, heat and
496 sonication as described above. Polyubiquitinated proteins were visualized by
497 immunoblotting for ubiquitin (Millipore Sigma 05-994, clone P4D1-A11), and actin
498 (Millipore Sigma MAB1501R) and tubulin (Abcam ab6160) was used as loading control.

499

500 **RNA preparation and analysis**

501 Approximately 3,000 nematodes from synchronized populations were cultured at 20 °C
502 or 25 °C per independent replicate, with three or four biological replicates used for the
503 qPCR and RNA-seq experiments. Animals were fed *E. coli* OP50 until reaching adulthood
504 and then transferred to plates seeded with either control bacteria or bacteria expressing
505 dsRNA, as previously described [43]. Adult nematodes were separated from the progeny

506 by collection in M9 buffer followed by gravity sedimentation for 2 min, and were
507 transferred daily to fresh RNAi plates until the final day of collection. After 48 or 72 hours
508 of RNAi exposure, worms were collected with M9, pelleted, frozen at −80 °C, and used
509 for RNA extraction. Total RNA was isolated using TRIzol reagent and subsequently
510 purified with the Direct-zol RNA MiniPrep kit (Zymo Research). RNA concentration was
511 determined by spectrophotometry using a TapeStation (Agilent). For qPCR analyses, 1
512 µg of RNA per sample was reverse-transcribed into cDNA, and transcript levels were
513 quantified as previously described [11] using a QuantStudio5 apparatus (Applied
514 Biosystems). Primer sequences used for qPCR analyses in this study are listed in
515 **Supplementary Table S4.** Statistical analyses were performed using GraphPad Prism
516 10 (GraphPad Software).
517

518 **RNA sequencing and differential gene expression analyses**

519 Library construction and next-generation sequencing (NGS) were performed by
520 polyadenylate selection and Illumina HiSeq methods (Genewiz-Azenta). Genes with a
521 minimum of 10 read counts in 4 samples (the number of biological replicates per
522 condition) were included in the analysis. The R package DESeq2 [69] was used to test
523 genes for differential expression and those with a false discovery rate of < 0.05 and fold
524 change > 2-fold were considered significant. GO enrichment analysis was conducted
525 using WormCat 2.0 [70] and heatmaps of gene expression were created using the R
526 package ComplexHeatmap [71].
527

528 **Germline extraction and immunofluorescence**

529 For immunofluorescence staining, adult worms were dissected in 1x PBS on a coverslip.
530 Coverslips were inverted onto poly-L-lysine–coated slides, snap-frozen at −80 °C, and
531 subjected to freeze-crack. Slides were immersed in cold methanol for 1 min and fixed for
532 30 min in a humid chamber in 1x PBS, 0.08 M HEPES (pH 6.9), 1.6 mM $MgSO_4$, 0.8 mM
533 EGTA, and 3.7% paraformaldehyde. Slides were washed three times in PBST (1x PBS,
534 0.1% Tween 20), blocked for 1 hr in PBST containing 3% BSA, and incubated overnight
535 at 4 °C with primary antibodies diluted in PBST with 1% BSA. Primary antibodies used
536 were anti-ubiquitin (Invitrogen, MA1-10035; 1:100), and anti-GRP78/HSPA5 (Novus
537 Biologicals, NBP1-06274; 1:200). Secondary Alexa Fluor 555-conjugated goat anti-
538 mouse (A32727, Life Technologies) and Alexa Fluor 647-conjugated goat anti-rabbit
539 secondary antibodies (111-605-003, Jackson ImmunoResearch) at 1:200 were incubated
540 for 1 hr at room temperature. Slides were washed in PBST, counterstained with DAPI,
541 mounted in Vectashield, sealed, and stored at −20 °C until imaging on a FV3000 confocal
542 microscope (Olympus).
543

544 **Computational analysis of RDE-1 and SID-1 structures**

545 The three-dimensional structures of the *Caenorhabditis elegans* proteins *rde-1* and *sid-1*
546 were obtained from public databases. The predicted structure of *rde-1* was retrieved from
547 the Alphafold protein structure database (https://alphafold.ebi.ac.uk/), using the model
548 AF-G5EEH0-F1-v6, corresponding to UniProt accession G5EEH0. The structure of *sid-1*
549 was obtained from the Protein Data Bank (PDB), using 8XC1, corresponding to the
550 dsRNA-bound form. Based on the amino acids sequence, point mutations were
551 introduced using AlphaFold Server (https://alphafoldserver.com/). The mutants *rde-1*

552 (E414K), *sid-1* (D130N), and *sid-1* (S536I) were generated. Native and mutant structures
553 were subsequently visualized and analyzed using UCSF ChimeraX
554 (https://www.cgl.ucsf.edu/chimerax/).
555

556 **ACKNOWLEDGEMENTS**

557 We would like to thank Dr. Brad Morrison (Boise State University), Dr. Eric Allain and
558 Sophie Landry (Université de Moncton), as well as Karine Blais for their feedback. We
559 are grateful to the Malene Hansen laboratory (Buck Institute for Research on Aging) for
560 sharing the N2 wild-type, MAH85, MAH677, AGD 635, AGD 637 and AGD639 used in this
561 study. We would like to thank Dr. Patrick Narbonne (UQTR) for helping perform tissue
562 extraction and immunofluorescence analyses. NSMDS performed lifespan analyses,
563 structural analyses and mRNA extractions. CB performed lifespan analyses and tissue-
564 specific RNAi studies. AO performed germline extraction and analyses. LH analyzed RNA
565 sequencing data. SK performed lifespan analyses. SD and STD conducted longitudinal
566 polyubiquitinated protein analyses. LRL designed the study, performed protein and gene
567 expression analyses, and tissue-specific RNAi analyses, and wrote the manuscript. All
568 co-authors edited the manuscript. No AI-assisted technologies were used in the writing of
569 this manuscript.
570

571 This work was funded by a Natural Sciences and Engineering Research Council of
572 Canada (NSERC) Discovery Grant, a Project Grant from Canadian Institutes of Health
573 Research (CIHR 519531) and a Research Chair in Precision Medicine (J.-Louis Lévesque
574 Foundation – NB Research) to LRL.

575

576 **DECLARATION OF INTERESTS**

577 The authors declare no competing interest.

578

579 **FIGURE LEGENDS**

580 **Figure 1. Levels of RNAi-defectiveness vary widely and in a temperature-dependent**
581 **manner across *rde-1* and *sid-1* mutants.** Lifespan of adult wild-type nematodes and
582 the mutant strains *rde-1 (ne300) V*, *rde-1(ne219) V*, *sid-1 (qt9) V*, and *sid-1 (pk3321)* were
583 analyzed at 20 °C **(A–E)** and 25 °C **(F–J)** and fed control bacteria or bacteria expressing
584 dsRNA for *ubq-1*. Details on lifespan analyses are available in Supplementary Tables S2
585 and S3.

586

587 **Figure 2. *In silico* structural analysis of *rde-1* and *sid-1* variants in *C. elegans*. (A)**
588 Structural superposition between wild-type *rde-1* (blue; AlphaFold Database) and the
589 *ne219*-associated E414K variant (green; AlphaFold server). While the global architecture
590 remains highly conserved, the focused view (right) illustrates the local environment
591 change where the acidic glutamic acid (E414, yellow) is replaced by the basic lysine
592 (K414, orange). **(B)** Impact of the *qt9* allele on the *sid-1* protein. The overlay shows the
593 S536I mutation (green; AlphaFold server) relative to the wild-type scaffold (blue; PDB:
594 8XC1). The detailed view highlights the substitution of the polar serine (S536, yellow) by
595 a hydrophobic isoleucine (I536, orange). **(C)** Architecture of the *sid-1(pk3321)* protein.
596 The model depicts the D130N substitution (green; AlphaFold server) aligned against the
597 wild-type reference (blue; PDB: 8XC1). The magnified inset highlights the shift at position

598 130, contrasting the wild-type aspartic acid (D130, yellow) with the mutant asparagine
599 (N130, orange). All molecular renderings and alignments were performed using UCSF
600 ChimeraX.
601
602 **Figure 3. Tissue-specific RNAi systems display varying degrees of specificity. (A)**
603 WT, *rde-1* and *sid-1* mutants as well as different strains with annotated tissue-specific
604 reconstitution for the intestine, hypodermis, muscle, germline or neurons were fed control
605 bacteria or bacteria expressing dsRNA against *elt-2* (intestine), *bli-3* (hypodermis)*, unc-*
606 *54* (muscle) or *xpo-1* (germline) from eggs to Day 1 of adulthood. In the case of partial
607 effects with *bli-3* silencing, animals that showed blisters were presented. Quantification of
608 displayed blisters (*bli-3* silencing) **(B)**, sluggishness (*unc-54* silencing) **(C)**, and vulvar
609 protrusions (*xpo-1* silencing) **(D)**. Three independent experiments (n=33-57 per
610 experiments).
611
612 **Figure 4. The germline is the most active site of proteasomal degradation in *C.***
613 ***elegans*.** Adult-only gene silencing of *rpn-6, pas-7* and *ubq-1* from day 1 to day 4 of
614 adulthood were performed at 25 °C in wild-type (**A**), *rde-1(ne219*) (**B**) as well as RDE-1
615 reconstituted strains in the intestine/germline (*nhx-2p*) (**C**), intestine/hypodermis/germline
616 (*lin-26p*) (**D**), intestine/germline (*mex-5p*) (**E**), and germline (*sun-1p*) (**F**).
617 Polyubiquitinated proteins (Ub) were visualized by immunoblotting and vitellogenin
618 proteins (* and **) are highlighted in the adjacent Ponceau staining. Representative
619 immunoblots of two independent experiments. Loading controls include immunoblotting
620 for tubulin (Tub) and actin.

621

622 **Figure 5. Vitellogenins located in the germline are major contributors of overall**
623 **polyubiquitinated protein levels. A.** Polyubiquitinated protein levels were visualized by
624 immunoblotting in Day 1 wild-type (WT), *fer-15(b26);fem-1(hc17)* and *glp-1(e2144)*
625 animals raised at 25 °C on OP50 *E. coli*. Three independent replicates SD +/- *ANOVA *:*
626 *P<0.05, **P<0.01*. **B.** Polyubiquitinated protein levels were visualized by immunoblotting
627 in day 1 and day 4 wild-type (WT) and *glp-1* animals raised at 25 °C on OP50 *E. coli*. **C.**
628 Adult-only silencing of *rpn-6, pas-7* and *ubq-1* in *glp-1* mutants raised at 25°C on OP50
629 *E. coli*. **D.** Adult-only silencing of *rpn-6* and *ubq-1* from Day 1 to Day 5 in VIT-2::GFP
630 expressing animals. **E.** Adult-only silencing of *rme-2* and *vit-1* from Day 1 to Day 4 in wild-
631 type animals. **F.** Extracted germline from Day 3 wild-type animals fed control bacteria or
632 bacteria expressing dsRNA against *ubq-1* from Day 1 of adulthood were visualized by
633 immunofluorescence using antibodies against ubiquitin, ER-resident GRP78 and DAPI
634 (nucleus).

635

636 **Figure 6. UBQ-1 is required for the active transcription of highly-expressed genes.**
637 **(A)** Polyubiquitinated protein levels in Day 4 wild-type animals fed OP50 *E.* coli, control
638 bacteria or bacteria expressing dsRNA against *ubq-1.* Biological duplicates. **(B)** Wormcat
639 analysis of upregulated genes and **(C)** downregulated genes in animals subjected to *ubq-*
640 *1* silencing from Day 1 to Day 4 of adulthood **(D)** Top 50 highest expressed genes with
641 significant downregulated expression from *ubq-1* silencing include marked
642 downregulation of vitellogenin genes. Details on global expression changes are available
643 in Supplementary Figure S2B and Supplementary Data S1.

644 **REFERENCES**

645 1. Fire, A., et al., *Potent and specific genetic interference by double-stranded RNA*
646 *in Caenorhabditis elegans.* Nature, 1998. **391**(6669): p. 806-11.
647 2. Kamath, R.S., et al., *Systematic functional analysis of the Caenorhabditis*
648 *elegans genome using RNAi.* Nature, 2003. **421**(6920): p. 231-7.
649 3. Rual, J.F., et al., *Toward improving Caenorhabditis elegans phenome mapping*
650 *with an ORFeome-based RNAi library.* Genome Res, 2004. **14**(10B): p. 2162-8.
651 4. Hansen, M., et al., *New genes tied to endocrine, metabolic, and dietary*
652 *regulation of lifespan from a Caenorhabditis elegans genomic RNAi screen.*
653 PLoS Genet, 2005. **1**(1): p. 119-28.
654 5. Hamilton, B., et al., *A systematic RNAi screen for longevity genes in C. elegans.*
655 Genes Dev, 2005. **19**(13): p. 1544-55.
656 6. Kenyon, C.J., *The genetics of ageing.* Nature, 2010. **464**(7288): p. 504-12.
657 7. Lapierre, L.R. and M. Hansen, *Lessons from C. elegans: signaling pathways for*
658 *longevity.* Trends Endocrinol Metab, 2012. **23**(12): p. 637-44.
659 8. Tabara, H., et al., *The rde-1 gene, RNA interference, and transposon silencing in*
660 *C. elegans.* Cell, 1999. **99**(2): p. 123-32.
661 9. Winston, W.M., C. Molodowitch, and C.P. Hunter, *Systemic RNAi in C. elegans*
662 *requires the putative transmembrane protein SID-1.* Science, 2002. **295**(5564): p.
663 2456-9.
664 10. Stefanakis, N., I. Carrera, and O. Hobert, *Regulatory Logic of Pan-Neuronal*
665 *Gene Expression in C. elegans.* Neuron, 2015. **87**(4): p. 733-50.

666 11. Wong, S.Q., et al., *Neuronal HLH-30/TFEB modulates peripheral mitochondrial*
667 *fragmentation to improve thermoresistance in Caenorhabditis elegans.* Aging
668 Cell, 2023. **22**(3): p. e13741.
669 12. Watts, J.S., et al., *New Strains for Tissue-Specific RNAi Studies in*
670 *Caenorhabditis elegans.* G3 (Bethesda), 2020. **10**(11): p. 4167-4176.
671 13. Gahlot, S. and J. Singh, *Caenorhabditis elegans neuronal RNAi does not render*
672 *other tissues refractory to RNAi.* Proc Natl Acad Sci U S A, 2024. **121**(22): p.
673 e2401096121.
674 14. Kumsta, C. and M. Hansen, *C. elegans rrf-1 mutations maintain RNAi efficiency*
675 *in the soma in addition to the germline.* PLoS One, 2012. **7**(5): p. e35428.
676 15. Calixto, A., et al., *Enhanced neuronal RNAi in C. elegans using SID-1.* Nat
677 Methods, 2010. **7**(7): p. 554-9.
678 16. Wolkow, C.A., et al., *Regulation of C. elegans life-span by insulin like signaling in*
679 *the nervous system.* Science, 2000. **290**(5489): p. 147-50.
680 17. Libina, N., J.R. Berman, and C. Kenyon, *Tissue-specific activities of C. elegans*
681 *DAF-16 in the regulation of lifespan.* Cell, 2003. **115**(4): p. 489-502.
682 18. Zhang, Y.P., et al., *Intestine-specific removal of DAF-2 nearly doubles lifespan in*
683 *Caenorhabditis elegans with little fitness cost.* Nat Commun, 2022. **13**(1): p.
684 6339.
685 19. Collins, G.A. and A.L. Goldberg, *The Logic of the 26S Proteasome.* Cell, 2017.
686 **169**(5): p. 792-806.
687 20. Walther, D.M., et al., *Widespread Proteome Remodeling and Aggregation in*
688 *Aging C. elegans.* Cell, 2015. **161**(4): p. 919-32.

689 21. Ben-Zvi, A., E.A. Miller, and R.I. Morimoto, *Collapse of proteostasis represents*
690 *an early molecular event in Caenorhabditis elegans aging.* Proc Natl Acad Sci U
691 S A, 2009. **106**(35): p. 14914-9.
692 22. Vecchi, G., et al., *Proteome-wide observation of the phenomenon of life on the*
693 *edge of solubility.* Proc Natl Acad Sci U S A, 2020. **117**(2): p. 1015-1020.
694 23. Vilchez, D., et al., *RPN-6 determines C. elegans longevity under proteotoxic*
695 *stress conditions.* Nature, 2012. **489**(7415): p. 263-8.
696 24. Keith, S.A., et al., *Graded Proteasome Dysfunction in Caenorhabditis elegans*
697 *Activates an Adaptive Response Involving the Conserved SKN-1 and ELT-2*
698 *Transcription Factors and the Autophagy-Lysosome Pathway.* PLoS Genet, 2016.
699 **12**(2): p. e1005823.
700 25. Mills, J., et al., *Combined Nucleotide and Protein Extractions in Caenorhabditis*
701 *elegans.* J Vis Exp, 2019(145).
702 26. Stringham, E.G., D. Jones, and E.P. Candido, *Expression of the polyubiquitin-*
703 *encoding gene (ubq-1) in transgenic Caenorhabditis elegans.* Gene, 1992.
704 **113**(2): p. 165-73.
705 27. Hirsh, D. and R. Vanderslice, *Temperature-sensitive developmental mutants of*
706 *Caenorhabditis elegans.* Dev Biol, 1976. **49**(1): p. 220-35.
707 28. Miller, H., et al., *Genetic interaction with temperature is an important determinant*
708 *of nematode longevity.* Aging Cell, 2017. **16**(6): p. 1425-1429.
709 29. Stroustrup, N., et al., *The temporal scaling of Caenorhabditis elegans ageing.*
710 Nature, 2016. **530**(7588): p. 103-7.

711 30. Goddard, T.D., et al., *UCSF ChimeraX: Meeting modern challenges in*
712 *visualization and analysis.* Protein Sci, 2018. **27**(1): p. 14-25.
713 31. Watts, J.S., et al., *New Strains for Tissue-Specific RNAi Studies in*
714 *Caenorhabditis elegans.* G3 (Bethesda), 2020.
715 32. Yigit, E., et al., *Analysis of the C. elegans Argonaute family reveals that distinct*
716 *Argonautes act sequentially during RNAi.* Cell, 2006. **127**(4): p. 747-57.
717 33. Espelt, M.V., et al., *Oscillatory Ca2+ signaling in the isolated Caenorhabditis*
718 *elegans intestine: role of the inositol-1,4,5-trisphosphate receptor and*
719 *phospholipases C beta and gamma.* J Gen Physiol, 2005. **126**(4): p. 379-92.
720 34. Qadota, H., et al., *Establishment of a tissue-specific RNAi system in C. elegans.*
721 Gene, 2007. **400**(1-2): p. 166-73.
722 35. Marre, J., E.C. Traver, and A.M. Jose, *Extracellular RNA is transported from one*
723 *generation to the next in Caenorhabditis elegans.* Proc Natl Acad Sci U S A,
724 2016. **113**(44): p. 12496-12501.
725 36. Zou, L., et al., *Construction of a germline-specific RNAi tool in C. elegans.* Sci
726 Rep, 2019. **9**(1): p. 2354.
727 37. Liu, L., C. Ruediger, and M. Shapira, *Integration of Stress Signaling in*
728 *Caenorhabditis elegans Through Cell-Nonautonomous Contributions of the JNK*
729 *Homolog KGB-1.* Genetics, 2018. **210**(4): p. 1317-1328.
730 38. Gelino, S., et al., *Intestinal Autophagy Improves Healthspan and Longevity in C.*
731 *elegans during Dietary Restriction.* PLoS Genet, 2016. **12**(7): p. e1006135.

732 39. McGhee, J.D., et al., *ELT-2 is the predominant transcription factor controlling*
733 *differentiation and function of the C. elegans intestine, from embryo to adult.* Dev
734 Biol, 2009. **327**(2): p. 551-65.
735 40. Edens, W.A., et al., *Tyrosine cross-linking of extracellular matrix is catalyzed by*
736 *Duox, a multidomain oxidase/peroxidase with homology to the phagocyte*
737 *oxidase subunit gp91phox.* J Cell Biol, 2001. **154**(4): p. 879-91.
738 41. Moerman, D.G., et al., *Mutations in the unc-54 myosin heavy chain gene of*
739 *Caenorhabditis elegans that alter contractility but not muscle structure.* Cell,
740 1982. **29**(3): p. 773-81.
741 42. Silvestrini, M.J., et al., *Nuclear Export Inhibition Enhances HLH-30/TFEB Activity,*
742 *Autophagy, and Lifespan.* Cell Rep, 2018. **23**(7): p. 1915-1921.
743 43. Kumar, A.V., et al., *Exportin 1 modulates life span by regulating nucleolar*
744 *dynamics via the autophagy protein LGG-1/GABARAP.* Sci Adv, 2022. **8**(13): p.
745 eabj1604.
746 44. Lapierre, L.R., et al., *The TFEB orthologue HLH-30 regulates autophagy and*
747 *modulates longevity in Caenorhabditis elegans.* Nat Commun, 2013. **4**: p. 2267.
748 45. Hsu, A.L., C.T. Murphy, and C. Kenyon, *Regulation of aging and age-related*
749 *disease by DAF-16 and heat-shock factor.* Science, 2003. **300**(5622): p. 1142-5.
750 46. Kenyon, C., et al., *A C. elegans mutant that lives twice as long as wild type.*
751 Nature, 1993. **366**(6454): p. 461-4.
752 47. Davy, A., et al., *A protein-protein interaction map of the Caenorhabditis elegans*
753 *26S proteasome.* EMBO Rep, 2001. **2**(9): p. 821-8.

754 48. Grant, B. and D. Hirsh, *Receptor-mediated endocytosis in the Caenorhabditis*
755 *elegans oocyte.* Mol Biol Cell, 1999. **10**(12): p. 4311-26.
756 49. Seah, N.E., et al., *Autophagy-mediated longevity is modulated by lipoprotein*
757 *biogenesis.* Autophagy, 2016. **12**(2): p. 261-72.
758 50. Steinbaugh, M.J., et al., *Lipid-mediated regulation of SKN-1/Nrf in response to*
759 *germ cell absence.* Elife, 2015. **4**.
760 51. Koyuncu, S., et al., *Rewiring of the ubiquitinated proteome determines ageing in*
761 *C. elegans.* Nature, 2021. **596**(7871): p. 285-290.
762 52. Waddell, B.M. and C.W. Wu, *Mutant alleles of the Caenorhabditis elegans rde-1*
763 *gene identified through chemical mutagenesis of an snRNA misprocessing*
764 *reporter.* G3 (Bethesda), 2025. **15**(7).
765 53. Camara, H., et al., *Tissue-specific overexpression of systemic RNA interference*
766 *components limits lifespan in C. elegans.* Gene, 2024. **895**: p. 148014.
767 54. Babin, P.J., et al., *Apolipophorin II/I, apolipoprotein B, vitellogenin, and*
768 *microsomal triglyceride transfer protein genes are derived from a common*
769 *ancestor.* J Mol Evol, 1999. **49**(1): p. 150-60.
770 55. Lapierre, L.R., et al., *Amino acid sequences within the beta1 domain of human*
771 *apolipoprotein B can mediate rapid intracellular degradation.* J Lipid Res, 2004.
772 **45**(2): p. 366-77.
773 56. Cecchettini, A., et al., *Vitellin cleavage products are proteolytically degraded by*
774 *ubiquitination in stick insect embryos.* Micron, 2003. **34**(1): p. 39-48.
775 57. Kumar, A.V., et al., *Lipid droplets modulate proteostasis, SQST-1/SQSTM1*
776 *dynamics, and lifespan in C. elegans.* iScience, 2023. **26**(10): p. 107960.

58. Bohnert, K.A. and C. Kenyon, *A lysosomal switch triggers proteostasis renewal in the immortal C. elegans germ lineage.* Nature, 2017. **551**(7682): p. 629-633.

59. Eroglu, M., et al., *Noncanonical inheritance of phenotypic information by protein amyloids.* Nat Cell Biol, 2024. **26**(10): p. 1712-1724.

60. Kern, C.C., et al., *C. elegans feed yolk to their young in a form of primitive lactation.* Nat Commun, 2021. **12**(1): p. 5801.

61. Altin, S., et al., *Ubiquitin precursor with C-terminal extension promotes proteostasis and longevity.* Mol Cell, 2025. **85**(19): p. 3677-3693 e7.

62. Papaevgeniou, N. and N. Chondrogianni, *The ubiquitin proteasome system in Caenorhabditis elegans and its regulation.* Redox Biol, 2014. **2**: p. 333-47.

63. Johnston, S.C., et al., *Structural basis for the specificity of ubiquitin C-terminal hydrolases.* EMBO J, 1999. **18**(14): p. 3877-87.

64. Mattiroli, F. and L. Penengo, *Histone Ubiquitination: An Integrative Signaling Platform in Genome Stability.* Trends Genet, 2021. **37**(6): p. 566-581.

65. Mark, K.G. and M. Rape, *Ubiquitin-dependent regulation of transcription in development and disease.* EMBO Rep, 2021. **22**(4): p. e51078.

66. Rangaraju, S., et al., *Suppression of transcriptional drift extends C. elegans lifespan by postponing the onset of mortality.* Elife, 2015. **4**: p. e08833.

67. Janes, J., et al., *Chromatin accessibility dynamics across C. elegans development and ageing.* Elife, 2018. **7**.

68. Brenner, S., *The genetics of Caenorhabditis elegans.* Genetics, 1974. **77**(1): p. 71-94.

799 69. Love, M.I., W. Huber, and S. Anders, *Moderated estimation of fold change and*
800 *dispersion for RNA-seq data with DESeq2.* Genome Biol, 2014. **15**(12): p. 550.
801 70. Holdorf, A.D., et al., *WormCat: An Online Tool for Annotation and Visualization of*
802 *Caenorhabditis elegans Genome-Scale Data.* Genetics, 2020. **214**(2): p. 279-
803 294.
804 71. Gu, Z., R. Eils, and M. Schlesner, *Complex heatmaps reveal patterns and*
805 *correlations in multidimensional genomic data.* Bioinformatics, 2016. **32**(18): p.
806 2847-9.
807

Figure 1.

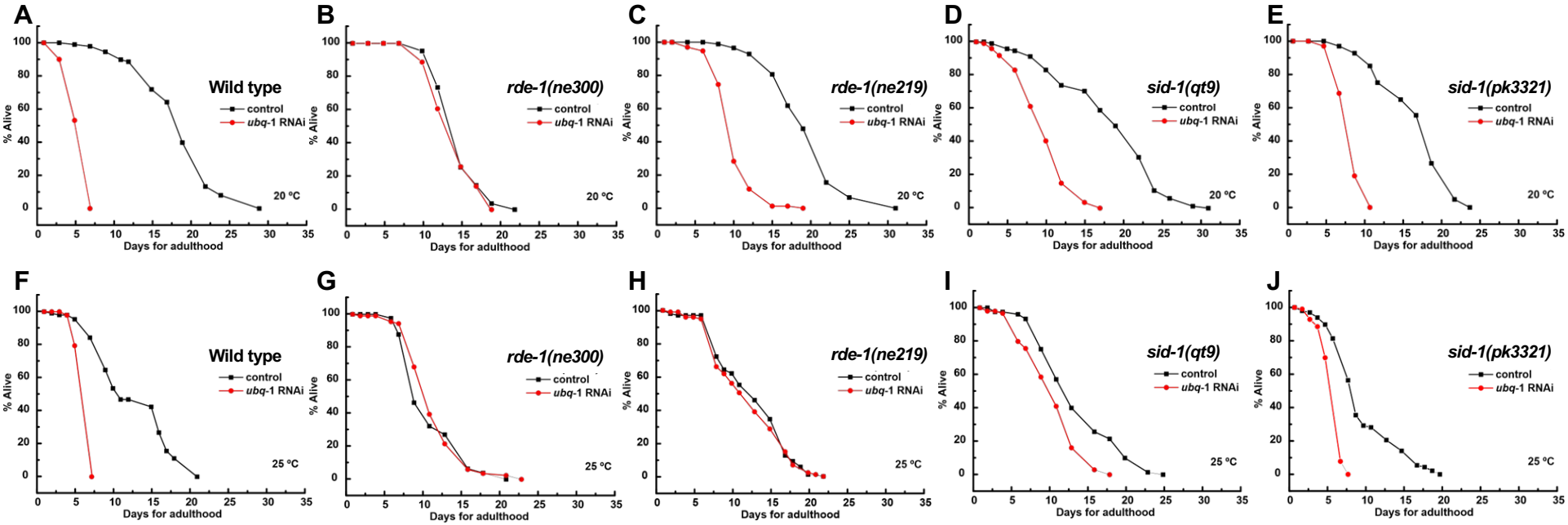
A
Wild type
control
ubq-1 RNAi
20 °C
% Alive
Days for adulthood
B
rde-1(ne300)
control
ubq-1 RNAi
20 °C
% Alive
Days for adulthood
C
rde-1(ne219)
control
ubq-1 RNAi
20 °C
% Alive
Days for adulthood
D
sid-1(qt9)
control
ubq-1 RNAi
20 °C
% Alive
Days for adulthood
E
sid-1(pk3321)
control
ubq-1 RNAi
20 °C
% Alive
Days for adulthood
F
Wild type
control
ubq-1 RNAi
25 °C
% Alive
Days for adulthood
G
rde-1(ne300)
control
ubq-1 RNAi
25 °C
% Alive
Days for adulthood
H
rde-1(ne219)
control
ubq-1 RNAi
25 °C
% Alive
Days for adulthood
I
sid-1(qt9)
control
ubq-1 RNAi
25 °C
% Alive
Days for adulthood
J
sid-1(pk3321)
control
ubq-1 RNAi
25 °C
% Alive
Days for adulthood

Figure 2

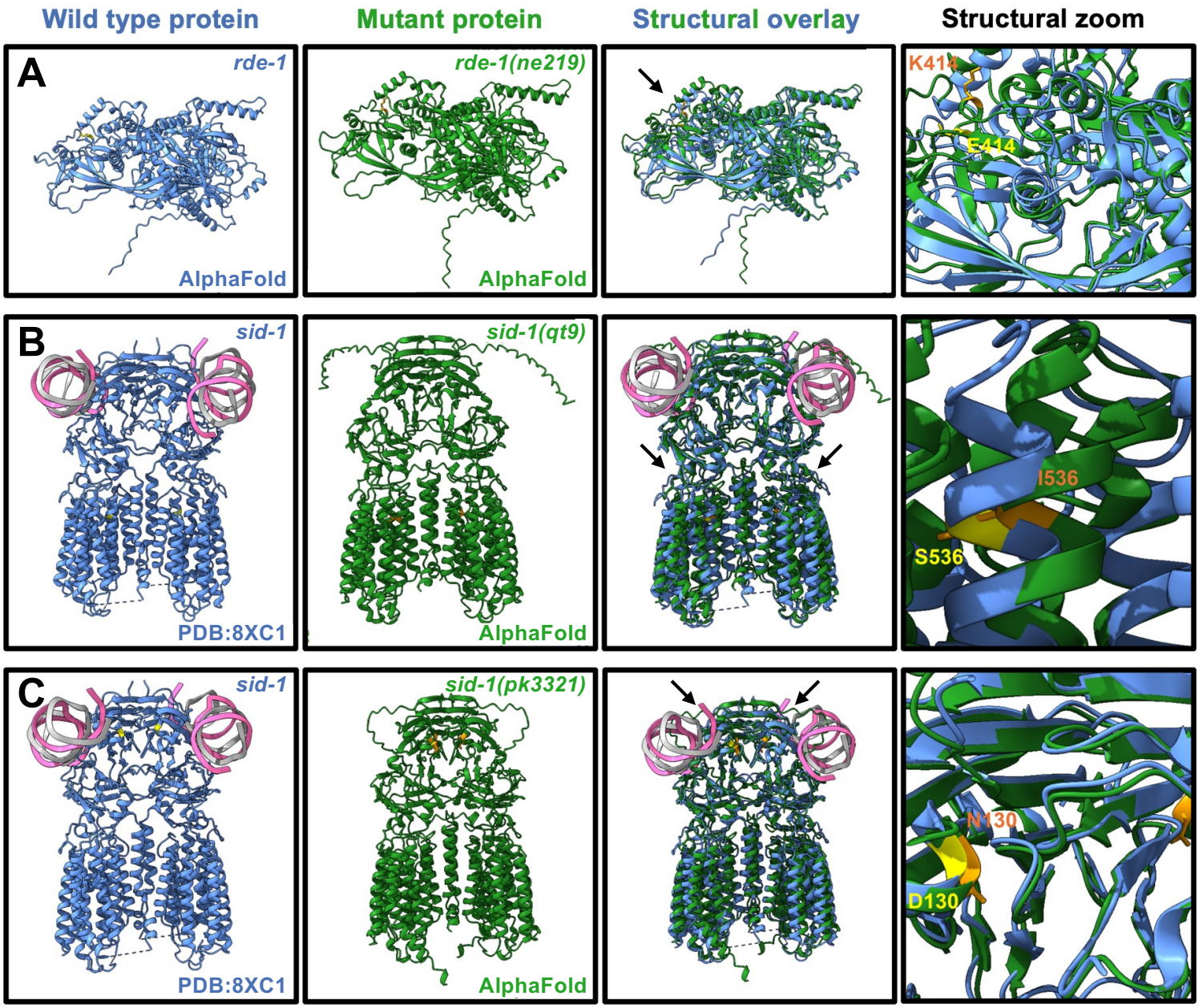
Wild type protein
Mutant protein
Structural overlay
Structural zoom
A
rde-1
AlphaFold
rde-1(ne219)
AlphaFold
K414
E414
B
sid-1
PDB:8XC1
sid-1(qt9)
AlphaFold
I536
S536
C
sid-1
PDB:8XC1
sid-1(pk3321)
AlphaFold
N130
D130

Figure 3

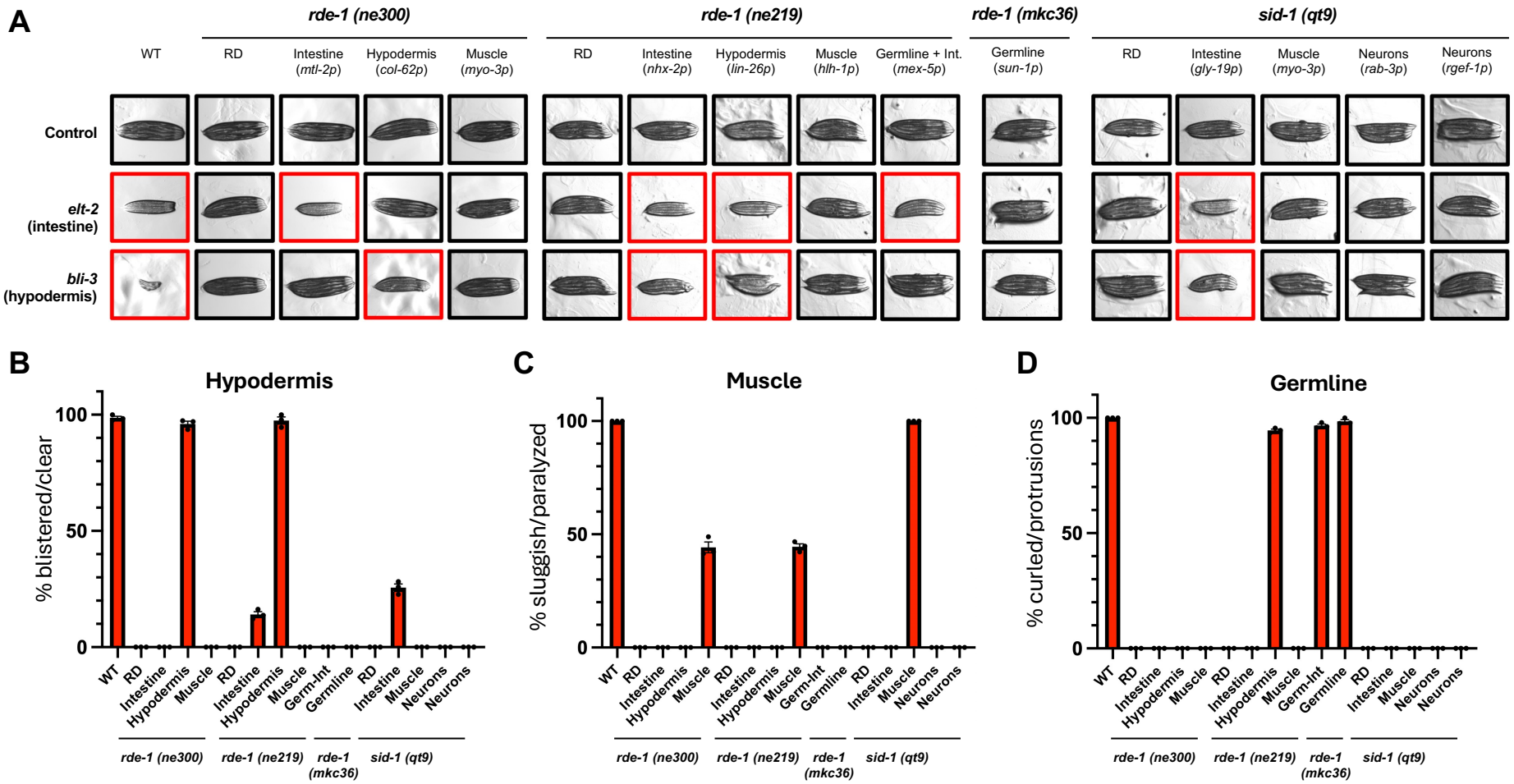
A
rde-1 (ne300)
rde-1 (ne219)
rde-1 (mkc36)
sid-1 (qt9)
WT
RD
Intestine (mtl-2p)
Hypodermis (col-62p)
Muscle (myo-3p)
RD
Intestine (nhx-2p)
Hypodermis (lin-26p)
Muscle (hlh-1p)
Germline + Int. (mex-5p)
Germline (sun-1p)
RD
Intestine (gly-19p)
Muscle (myo-3p)
Neurons (rab-3p)
Neurons (rgef-1p)
Control
elt-2 (intestine)
bli-3 (hypodermis)
B
Hypodermis
% blistered/clear
100
50
0
WT
RD
Intestine
Hypodermis
Muscle
RD
Intestine
Hypodermis
Muscle
Germ-Int
Germline
RD
Intestine
Muscle
Neurons
Neurons
rde-1 (ne300)
rde-1 (ne219)
rde-1 (mkc36)
sid-1 (qt9)
C
Muscle
% sluggish/paralyzed
100
50
0
WT
RD
Intestine
Hypodermis
Muscle
RD
Intestine
Hypodermis
Muscle
Germ-Int
Germline
RD
Intestine
Muscle
Neurons
Neurons
rde-1 (ne300)
rde-1 (ne219)
rde-1 (mkc36)
sid-1 (qt9)
D
Germline
% curled/protrusions
100
50
0
WT
RD
Intestine
Hypodermis
Muscle
RD
Intestine
Hypodermis
Muscle
Germ-Int
Germline
RD
Intestine
Muscle
Neurons
Neurons
rde-1 (ne300)
rde-1 (ne219)
rde-1 (mkc36)
sid-1 (qt9)

Figure 4

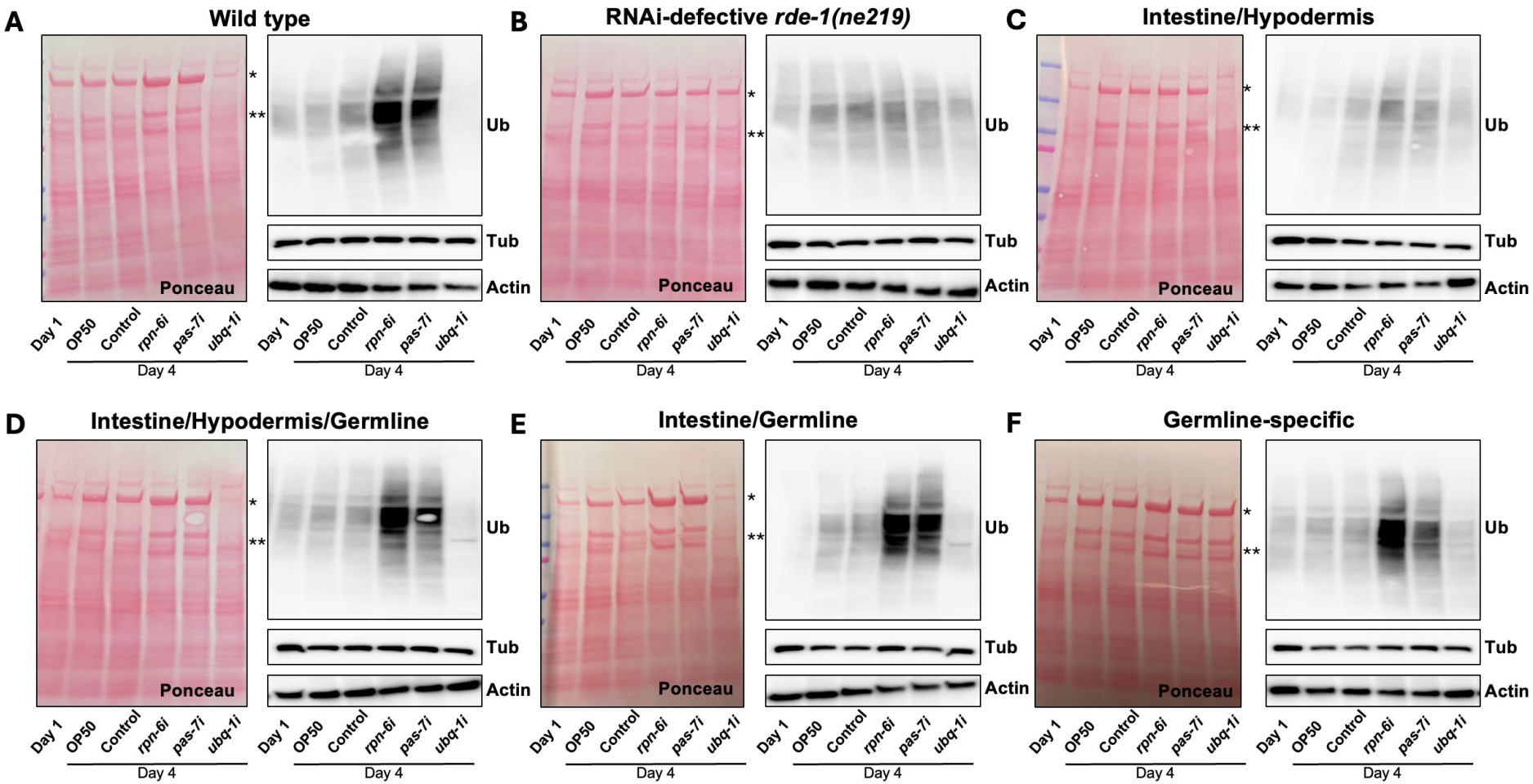
A
Wild type
B
RNAi-defective rde-1(ne219)
C
Intestine/Hypodermis
D
Intestine/Hypodermis/Germline
E
Intestine/Germline
F
Germline-specific
Ponceau
Ub
Tub
Actin
*
**
Day 1
OP50
Control
rpn-6i
pas-7i
ubq-1i
Day 4

Figure 5

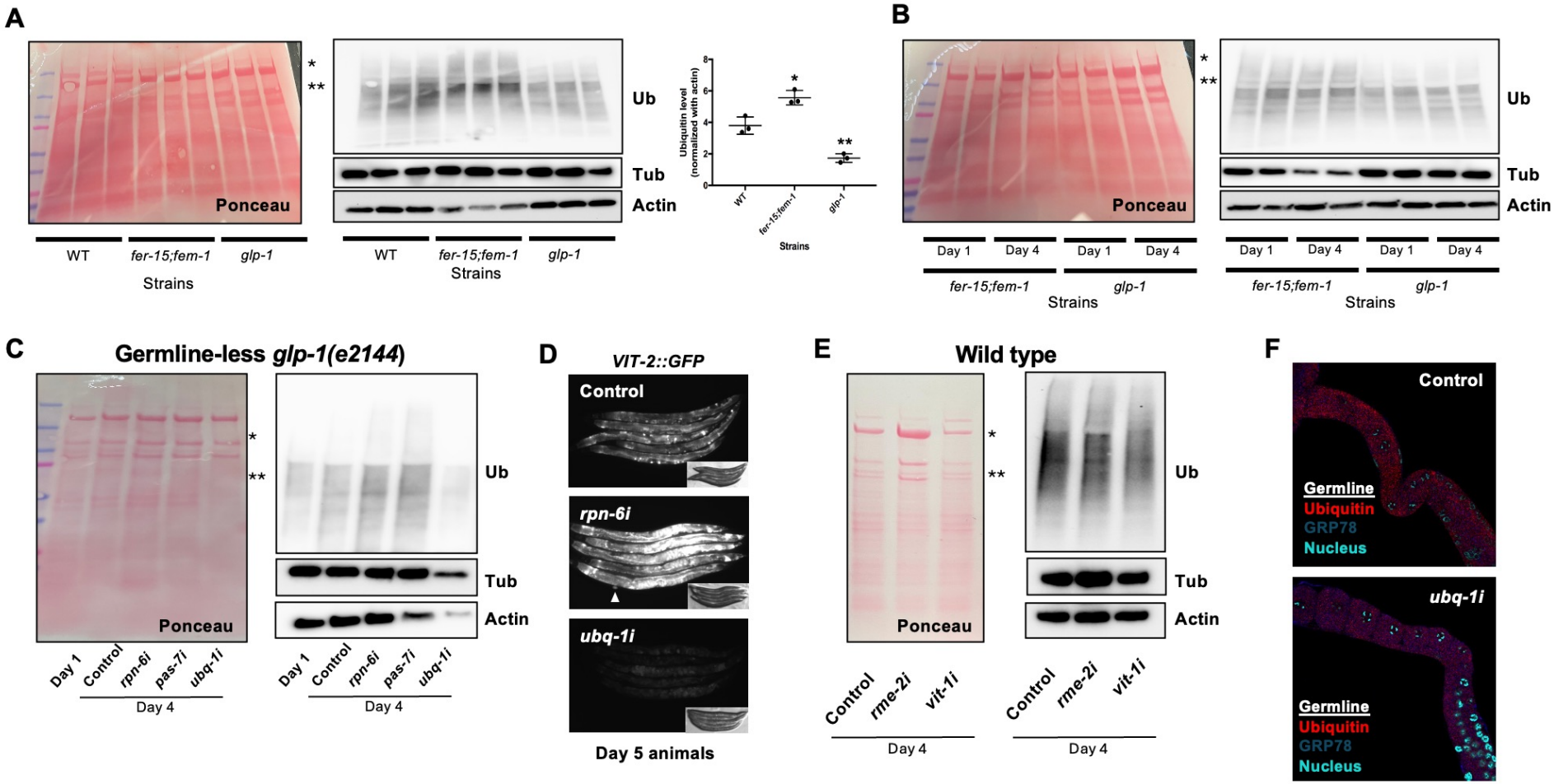
A
Ponceau
*
**
Ub
Tub
Actin
WT
fer-15;fem-1
glp-1
Strains
Ubiquitin level (normalized with actin)
B
Day 1
Day 4
C
Germline-less glp-1(e2144)
Control
rpn-6i
pas-7i
ubq-1i
D
VIT-2::GFP
Day 5 animals
E
Wild type
rme-2i
vit-1i
F
Germline
Ubiquitin
GRP78
Nucleus

Figure 6

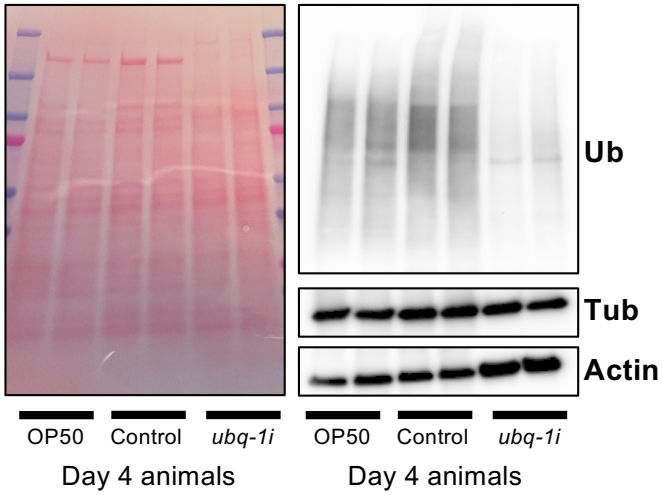
A
Ub
Tub
Actin
OP50
Control
ubq-1i
OP50
Control
ubq-1i
Day 4 animals
Day 4 animals

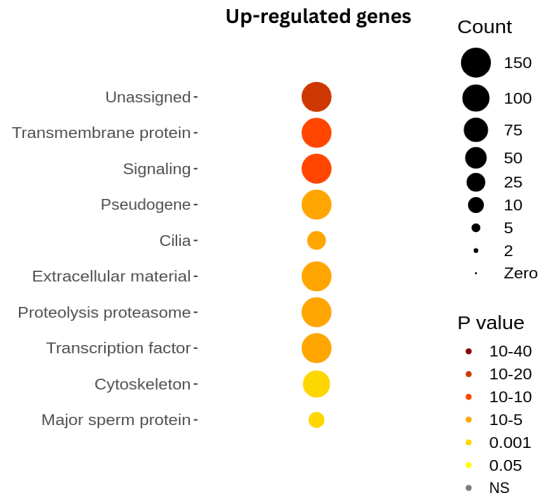
B
Up-regulated genes
Unassigned
Transmembrane protein
Signaling
Pseudogene
Cilia
Extracellular material
Proteolysis proteasome
Transcription factor
Cytoskeleton
Major sperm protein
Count
150
100
75
50
25
10
5
2
Zero
P value
10-40
10-20
10-10
10-5
0.001
0.05
NS

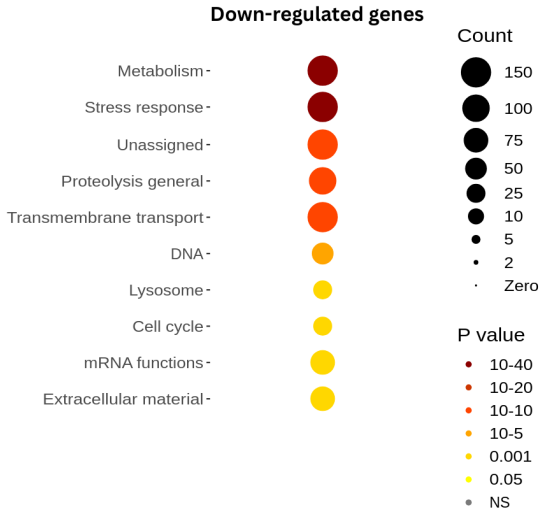
C
Down-regulated genes
Metabolism
Stress response
Unassigned
Proteolysis general
Transmembrane transport
DNA
Lysosome
Cell cycle
mRNA functions
Extracellular material
Count
150
100
75
50
25
10
5
2
Zero
P value
10-40
10-20
10-10
10-5
0.001
0.05
NS

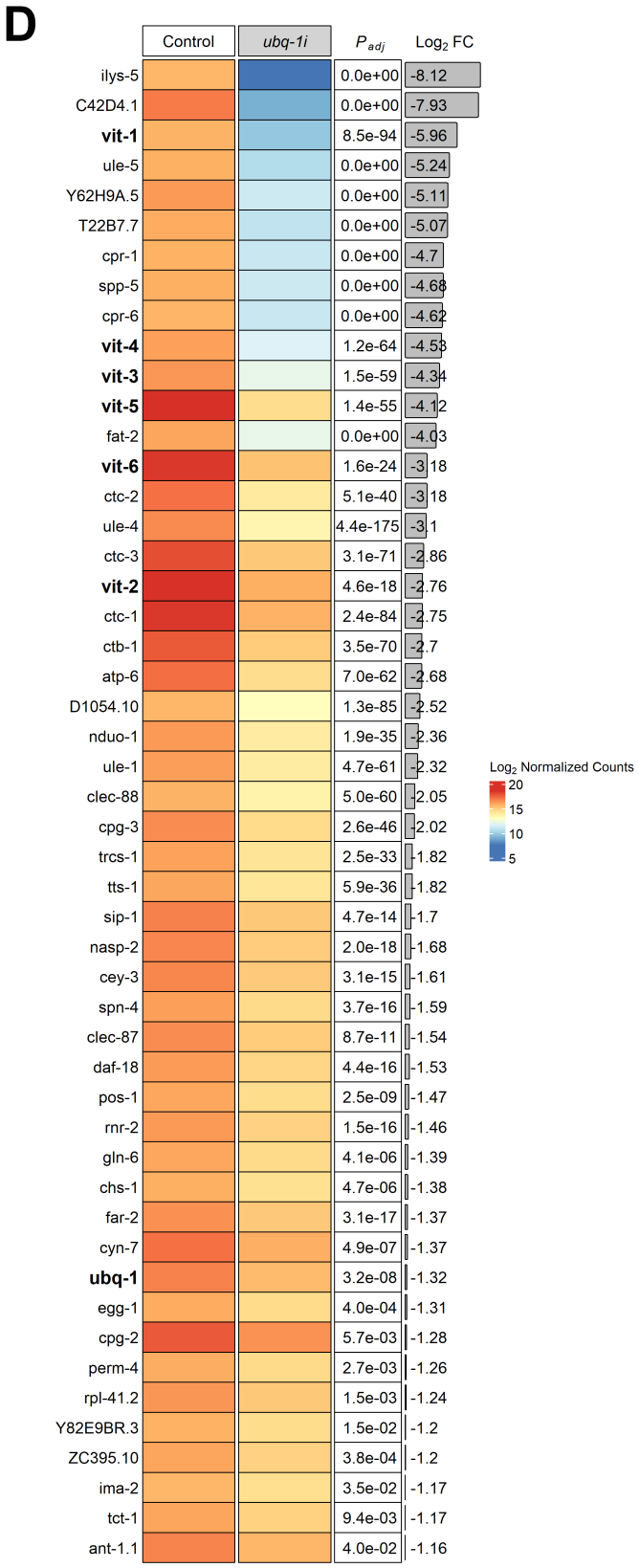
D
Control
ubq-1i
P adj
Log2 FC
ilys-5 0.0e+00 -8.12
C42D4.1 0.0e+00 -7.93
vit-1 8.5e-94 -5.96
ule-5 0.0e+00 -5.24
Y62H9A.5 0.0e+00 -5.11
T22B7.7 0.0e+00 -5.07
cpr-1 0.0e+00 -4.7
spp-5 0.0e+00 -4.68
cpr-6 0.0e+00 -4.62
vit-4 1.2e-64 -4.53
vit-3 1.5e-59 -4.34
vit-5 1.4e-55 -4.12
fat-2 0.0e+00 -4.03
vit-6 1.6e-24 -3.18
ctc-2 5.1e-40 -3.18
ule-4 4.4e-175 -3.1
ctc-3 3.1e-71 -2.86
vit-2 4.6e-18 -2.76
ctc-1 2.4e-84 -2.75
ctb-1 3.5e-70 -2.7
atp-6 7.0e-62 -2.68
D1054.10 1.3e-85 -2.52
nduo-1 1.9e-35 -2.36
ule-1 4.7e-61 -2.32
clec-88 5.0e-60 -2.05
cpg-3 2.6e-46 -2.02
trcs-1 2.5e-33 -1.82
tts-1 5.9e-36 -1.82
sip-1 4.7e-14 -1.7
nasp-2 2.0e-18 -1.68
cey-3 3.1e-15 -1.61
spn-4 3.7e-16 -1.59
clec-87 8.7e-11 -1.54
daf-18 4.4e-16 -1.53
pos-1 2.5e-09 -1.47
rnr-2 1.5e-16 -1.46
gln-6 4.1e-06 -1.39
chs-1 4.7e-06 -1.38
far-2 3.1e-17 -1.37
cyn-7 4.9e-07 -1.37
ubq-1 3.2e-08 -1.32
egg-1 4.0e-04 -1.31
cpg-2 5.7e-03 -1.28
perm-4 2.7e-03 -1.26
rpl-41.2 1.5e-03 -1.24
Y82E9BR.3 1.5e-02 -1.2
ZC395.10 3.8e-04 -1.2
ima-2 3.5e-02 -1.17
tct-1 9.4e-03 -1.17
ant-1.1 4.0e-02 -1.16
Log2 Normalized Counts
20
15
10
5